

TITLE: THE LOW-Q DIFFRACTOMETER AT THE LOS ALAMOS NEUTRON SCATTERING CENTER

AUTHOR(S): P. A. Seeger, LANSCE  
A. Williams, LANSCE  
J. Trewhella, LS-7

LA-UR--86-4387

DE87 003763

SUBMITTED TO: Conference Proceedings for the Ninth Meeting of the  
International Collaboration on Advanced Neutron Sources (ICANS)

### DISCLAIMER

This report was prepared as an account of work sponsored by an agency of the United States Government. Neither the United States Government nor any agency thereof, nor any of their employees, makes any warranty, express or implied, or assumes any legal liability or responsibility for the accuracy, completeness, or usefulness of any information, apparatus, product, or process disclosed, or represents that its use would not infringe privately owned rights. Reference herein to any specific commercial product, process, or service by trade name, trademark, manufacturer, or otherwise does not necessarily constitute or imply its endorsement, recommendation, or favoring by the United States Government or any agency thereof. The views and opinions of authors expressed herein do not necessarily state or reflect those of the United States Government or any agency thereof.

By acceptance of this article, the publisher recognizes that the U.S. Government retains a nonexclusive, royalty-free license to publish or reproduce the published form of this contribution, or to allow others to do so, for U.S. Government purposes.

The Los Alamos National Laboratory requests that the publisher identify this article as work performed under the auspices of the U.S. Department of Energy.

 Los Alamos National Laboratory  
Los Alamos, New Mexico 87545

**MASTER**

## THE LOW-Q DIFFRACTOMETER AT THE LOS ALAMOS NEUTRON SCATTERING CENTER

P. A. Seeger, A. Williams, and J. Trevhella

Los Alamos National Laboratory, Los Alamos, NM 87545, USA

### Abstract

Instrument criteria are presented for the Low-Q Diffractometer (LQD) at the Los Alamos Neutron Scattering Center (LANSCE), and a design is shown to meet these criteria. The collimator consists of multiple-aperture pinhole plates, and incorporates "dynamic gravity focusing" to center all wavelengths on the detector. Preliminary test results, making use of the Proton Storage Ring, a liquid hydrogen moderator, and two different position-sensitive detectors are shown.

### 1. Introduction

Since our report at the preceding ICANS meeting<sup>1)</sup>, considerable progress has been made in the implementation of the Low-Q Diffractometer (LQD) and its position-sensitive detectors. A prototype instrument was operated in December, 1985, using the liquid hydrogen moderator<sup>2)</sup> and an Anger camera<sup>3)</sup>. First tests of the almost-completed instrument were made in September, 1986, using a two-dimensional <sup>3</sup>He proportional counter. The LQD is being installed on flight path 10 (the northeast corner) in the existing experimental hall. With the Proton Storage Ring (PSR) operating at 24 Hz, the flight path of 12.65 m allows use of neutron wavelengths out to 13 Å before frame overlap, without the need for choppers or filters. An elevation view of the instrument is shown in fig. 1.

This flight path views a liquid hydrogen moderator which produces a neutron spectrum peaked at a wavelength of 2.4 Å but with usable flux from 0.3 to 15 Å. For design purposes when estimating the low-Q limit of the instrument we have chosen  $\lambda = 8$  Å to represent the maximum wavelength for obtaining statistically significant results.

The detector resolution and efficiency are assumed to be good enough not to affect optimization. For instance, the proposed larger Anger camera has an rms resolution better than 1.5 mm, and it will be digitized in bins 2.3 mm square. This will not contribute significantly to the resolution if the sample-to-detector distance is greater than 3 m. The <sup>3</sup>He detector, however, has an rms resolution of nearly 4 mm, and also somewhat lower

# FLIGHT PATH #10

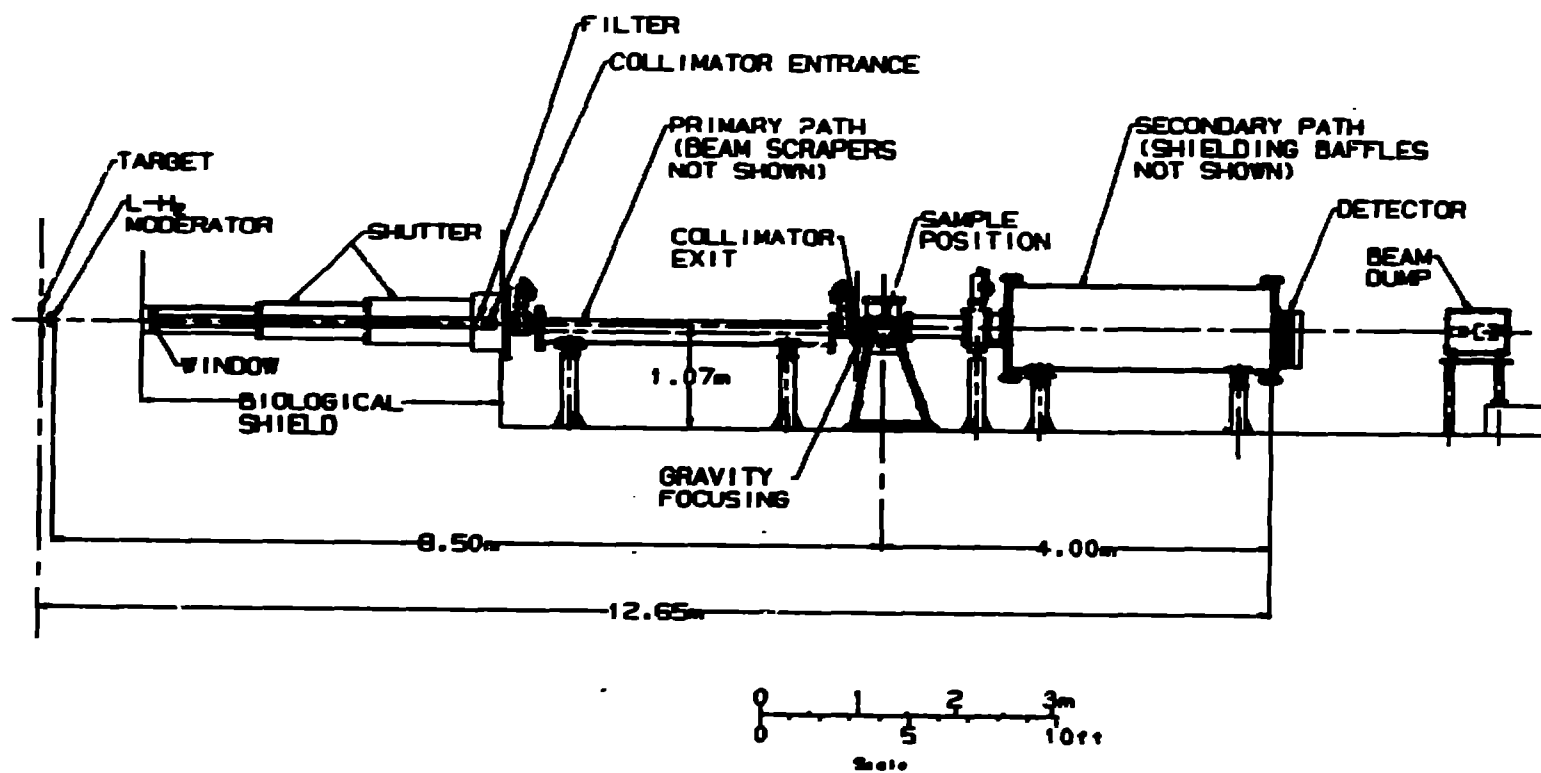


Fig. 1. Elevation view of the Low-Q Diffractometer.

efficiency than the Anger camera; we expect to use this detector only until the new and larger Anger camera is built.

## 2. Design Criteria

The parameter of interest in a small-angle experiment is the momentum transfer,  $hQ$ , which is inversely proportional to the wavelength and approximately proportional to the scattering angle. The primary requirement of the instrument is to be able to take statistically significant data at a minimum value of  $Q$  of the order  $Q_{\min} = 0.003 \text{ \AA}^{-1}$ . With  $\lambda_{\max} = 8 \text{ \AA}$ , the minimum scattering angle is

$$\theta_{\min} = \frac{\lambda_{\max} Q_{\min}}{2\pi} = 3.8 \text{ mrad}$$

We also require an rms resolution at least as good as 30% at  $Q_{\min}$ , so that the standard deviation of  $\theta$  must be

$$\sigma_{\theta} < 1.15 \text{ mrad.}$$

These angular criteria establish the relative sizes of the collimator apertures.

An obvious design goal is to maximize the counting rate of an experiment. Once the angular parameters are determined, however, there is very little which can be done to affect the flux on sample<sup>4)</sup>; for instance, if the instrument is shortened to gain flux by the  $1/R^2$  increase of solid angle, then the area of moderator seen at any point on the sample must be decreased by exactly the same factor to maintain resolution. For a given moderator surface brightness ( $n/\text{cm}^2/\text{ster}/s$ ), the only way to increase intensity is by increasing the sample size, up to the limit that the full moderator surface is being used. Since frame overlap (as well as the available space in the experimental hall) limits the scale factor by which the design can be multiplied, the only way to increase sample size is through use of multiple-aperture collimators.

The third criterion is to allow an extended dynamic range in  $Q$ , up to at least  $1.0 \text{ \AA}^{-1}$ . This is readily accomplished by utilizing a wide band of the pulsed source wavelength spectrum, and by using an area detector covering a reasonably large angular range. We will be able to record all wavelengths longer than  $0.3 \text{ \AA}$ , relying on time of flight to eliminate the power pulse. We have also allowed for the possibility of including a filter to eliminate the high-energy neutrons to reduce backgrounds for experiments using only long wavelengths.

### 3. Collimator Aperture Sizes

Optimization of the variance of the scattering angle due to moderator and sample collimation requires that<sup>5)</sup>

$$\overline{r_1^2} / \overline{r_2^2} = \left( \frac{L_1 + L_2}{L_2} \right)^2 ,$$

or that the root-mean-square radii of the moderator and sample are proportional to their respective distances from the detector, where  $L_1$  is the incident flight path length and  $L_2$  is the sample-to-detector distance. We choose path lengths based on practical considerations, and hunt for aperture sizes which satisfy the above criteria. If the result is unsatisfactory, we can modify the path lengths and repeat the procedure. Since the geometry is additionally complicated by the separation of the defining apertures from the source and sample, a Monte-Carlo code was run to evaluate and optimize the variance. A typical result (for  $L_1 = 8.75$  m and  $L_2 = 3.75$  m) is

$$R_1 = 5.47 \text{ mm}, \quad R_2 = 3.03 \text{ mm},$$

producing penumbra radii at the moderator and sample of

$$R_M = 16.2 \text{ mm}, \quad R_S = 3.6 \text{ mm} .$$

### 4. Multiple Apertures

These moderator and sample sizes do not take full advantage of the available source area. Multiple aperture sets, all converging to the same point at the detector, increase the intensity without affecting the resolution. Figure 2 illustrates a set of 7 holes to match the size of the moderator (120 mm x 120 mm) and to illuminate a sample 36 mm in diameter. Intermediate beam scraping baffles are required to prevent neutrons crossing from one imaginary tube to another in the multiaperture system. The "Primary Path" pipe in fig. 1 will contain a rotating assembly to allow three different collimators, probably with one, seven, and nineteen holes, respectively.

### 5. Dynamic Gravity Focusing

At 24 Hz, neutrons recorded at the end of the frame will have fallen 8.5 mm under the influence of gravity. Rather than increasing the size of the beam stop, we want to select the neutrons whose parabolic trajectories strike the detector at its center; the "Gravity Focusing" device indicated in fig. 1 does this by pushing the collimator exit aperture plate upward during each beam pulse. The maximum excursion (for 13 Å neutrons) is

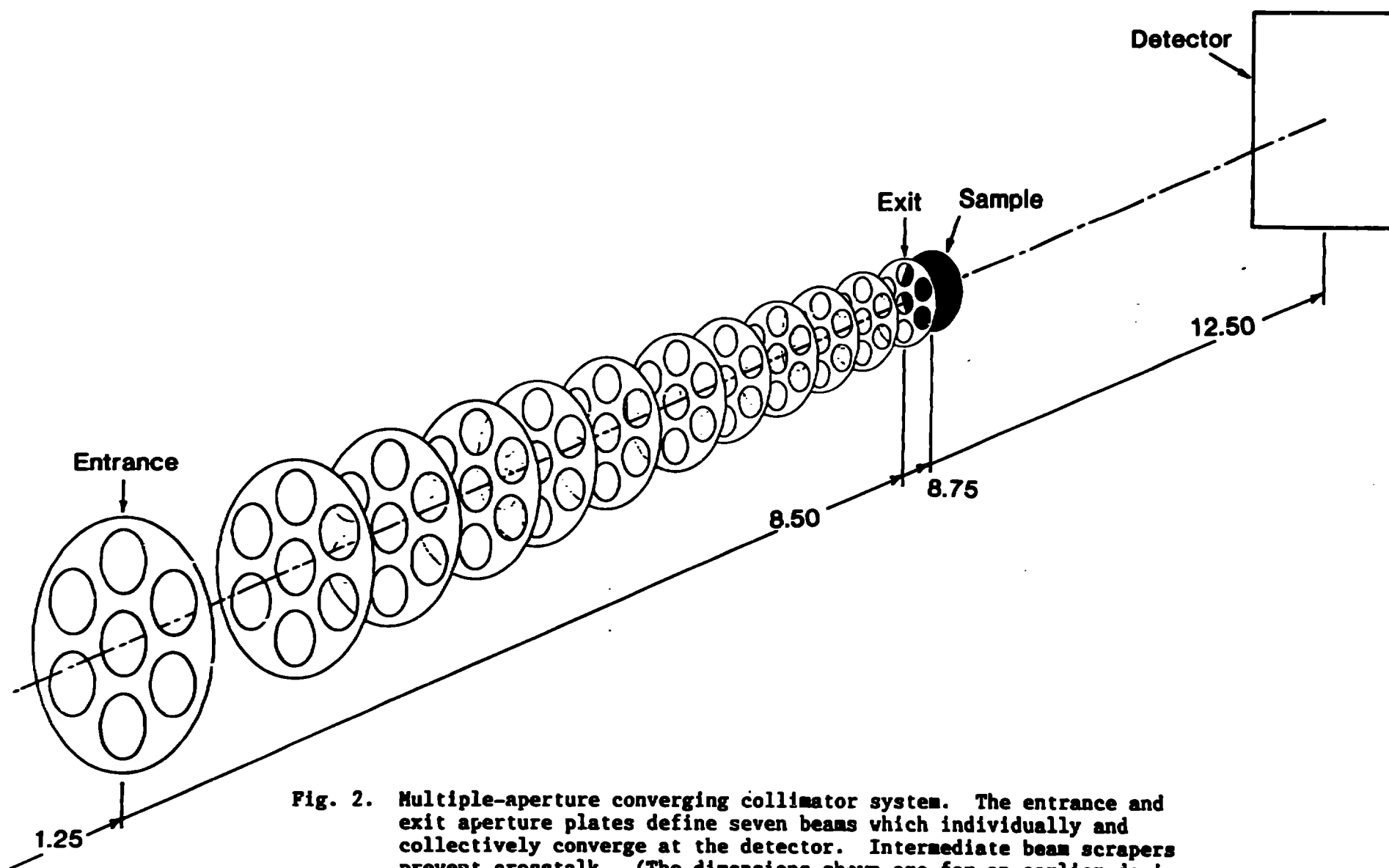


Fig. 2. Multiple-aperture converging collimator system. The entrance and exit aperture plates define seven beams which individually and collectively converge at the detector. Intermediate beam scrapers prevent crosstalk. (The dimensions shown are for an earlier design than fig. 1.)

0.82 mm. Without correction, the droop at the detector would be 4 mm. Also note that the beam-scraper apertures must be enlarged to include all the trajectories to be used.

The hydraulic servoamplifier system for the gravity focusing has been ordered, and we hope to have it working in early 1987.

## 6. Sample Chamber

The vacuum chamber at the sample position is 300 mm in diameter and 450 mm high. There are access flanges on the top, bottom, and both sides. A remotely controlled sample changer will be provided, as well as controlled humidity and temperature environments.

For experiments requiring larger or highly specialized environments, the sample chamber and the pipe spool attached to it may be removed, providing an open length of 1 m.

## 7. Detector

The detector represented in fig. 1 is an Anger camera. The 50-mm thick optical glass disperser plate is used as the vacuum window, so that there are no windows in front of the scintillator. The detector area (300 mm x 450 mm) is off-center to increase the dynamic range. A 9 x 7 array of photomultipliers detects about 700 photons from each neutron capture in the  $^6\text{Li}$ -loaded glass scintillator, and linear combinations of the signals identify the location of each individual event. Using our optimized encoding scheme<sup>6)</sup>, the time per event has been reduced (from the value of several  $\mu\text{s}$  in the standard Anger camera) to only 0.4  $\mu\text{s}$ . This is very significant because of the high instantaneous data rates expected at LANSCE. Furthermore, the encoding in different parts of the detector may be done in parallel, so that simultaneous events may be recorded.

The Anger camera is expected to meet our design requirements, but is still under development. As a temporary alternative detector, we have purchased a  $^3\text{He}$  position-sensitive proportional counter from the Risø National Laboratory in Denmark<sup>7)</sup>.

## 8. Test with Anger Camera.

In December, 1985, the LQD was assembled using a previously used shutter and collimator<sup>8)</sup> in order to test the liquid hydrogen moderator and also the behavior of the Anger camera when placed in the direct neutron beam. The new and old parts of the instrument were not well aligned with each other, however, and there was not enough memory to record the whole detector in two dimensions. Coupled with the (expected) early-time

saturation of the detector electronics, this made it impossible for us to measure the beam position or the detector resolution. The saturation has subsequently been improved by decreasing time constants in the photomultiplier preamplifiers. The detector did "survive" in the direct neutron beam (at 10  $\mu$ A proton current), and at times later than 2 ms gave a measurement of the flux from the liquid hydrogen moderator (fig. 3). This spectrum shows the peak of intensity at 14 meV (below which ortho hydrogen is transparent to neutrons), Bragg absorption edges in the aluminum vessel of the moderator, and a long-wavelength distribution which is similar to a Maxwellian.

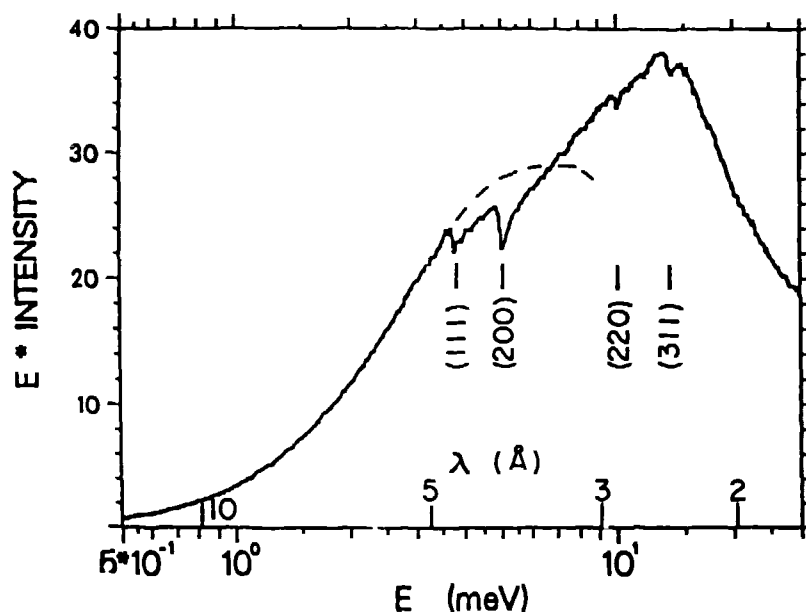


Fig. 3. Long-wavelength spectrum from the liquid hydrogen moderator. No corrections have been made for detector efficiency, or for absorption in the aluminum vessel. There is a quasi-Maxwellian tail corresponding to about 30 K, but the dominant feature is the peak at 14 meV resulting from transparency of ortho hydrogen.

## 9. Test with the $^3\text{He}$ Detector.

The instrument was reassembled in nearly its final form and another test run was made in September, 1986. The detector in this case was the newly acquired  $^3\text{He}$  detector from Risø. A beam stop of pressed  $^6\text{LiF}$ , 25-mm diameter by 30 mm long, was attached to the front of the detector. However we did not yet have the entrance aperture of the collimator installed, so the neutron beam was much larger and only 1/3 to 1/2 of the beam was intercepted by the beam stop. We placed about 10 cm of Pb at the sample position to attenuate the beam and to scatter neutrons into the full detector area.

The preamplifiers on the vertical dimension of the detector, purchased from Ordela, Inc., which were designed for use on position-sensitive



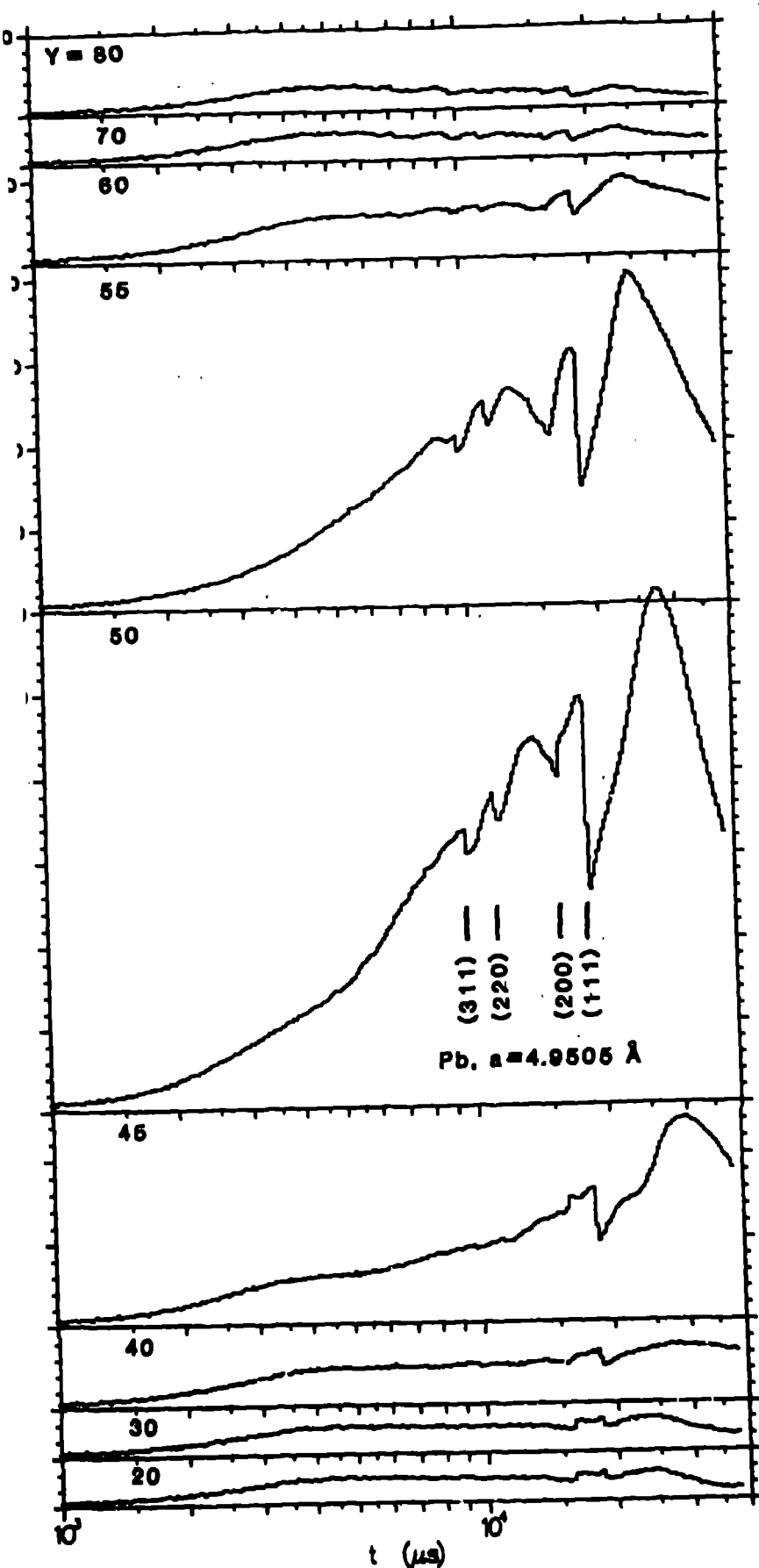
detectors, showed no signs of saturation at the time of the proton pulse. Unfortunately we had damaged the horizontal preamps, and an attempt to replace them with "standard" preamps failed because they saturated and remained dead for longer than the 38.6 ms counting frame. Thus although the data acquisition system was capable of recording a full 2-Mword histogram (283 time channels  $\times$  86 X-bins  $\times$  86 Y-bins), we were unable to encode the X position. Each value of Y represents a strip across the circular detector face. Figure 4 shows observed time spectra at several vertical positions for 8 hours of beam at 22  $\mu$ A. At Y = 50 there is a large contribution from the direct beam since it was larger than the stop. The first four Bragg edges of Pb are marked. At short wavelengths, the transmission of the Pb is 8%, and the other 92% of the beam is multiply scattered into  $4\pi$  ster. Figure 5 is a summation of the wavelength band from 1.2 to 2.8  $\text{\AA}$ , plotted vs. vertical position. A Gaussian has been drawn through the direct beam profile. At wavelengths longer than 5.7  $\text{\AA}$  we observe the full beam with only small-angle scattering, as illustrated in fig. 6 for a wavelength of 12  $\text{\AA}$ . Note that the beam center is considerably lower on the detector, due to gravity.

#### 10. Future Schedule.

The single-aperture collimator will be completed and a variety of calibration samples will be run in December, 1986. Guided by the results of those tests and the tests already performed, the instrument will be completed during the following six-month shutdown of LANSCE. The gravity focusing mechanism and the multiple-aperture collimators will be installed, a small scintillator monitor detector will be mounted at the center of the beam stop in front of the main detector, the new Anger camera will be built, and a filter will be designed to be placed before the collimator entrance aperture. New permanent shielding will be installed around the detector and around the collimator apertures. We will also be developing and adapting software to analyze the 1986 data and to be prepared for the 1987 run cycle. The instrument should be fully operational and ready for outside experimenters by the end of 1987.

#### Acknowledgments

The LQD would not be as well along as it is today without the help which has been received from colleagues at the IPNS and at ISIS, in the true spirit of ICANS. This work is supported by the U. S. Department of Energy.



x-ray diffraction spectra at various vertical positions, summed across horizontal extent of the detector. Each unit in Y is about 10 cm. There was 10 cm of Pb in the beam, leading to both large-angle scattering, and to strong Bragg effects.

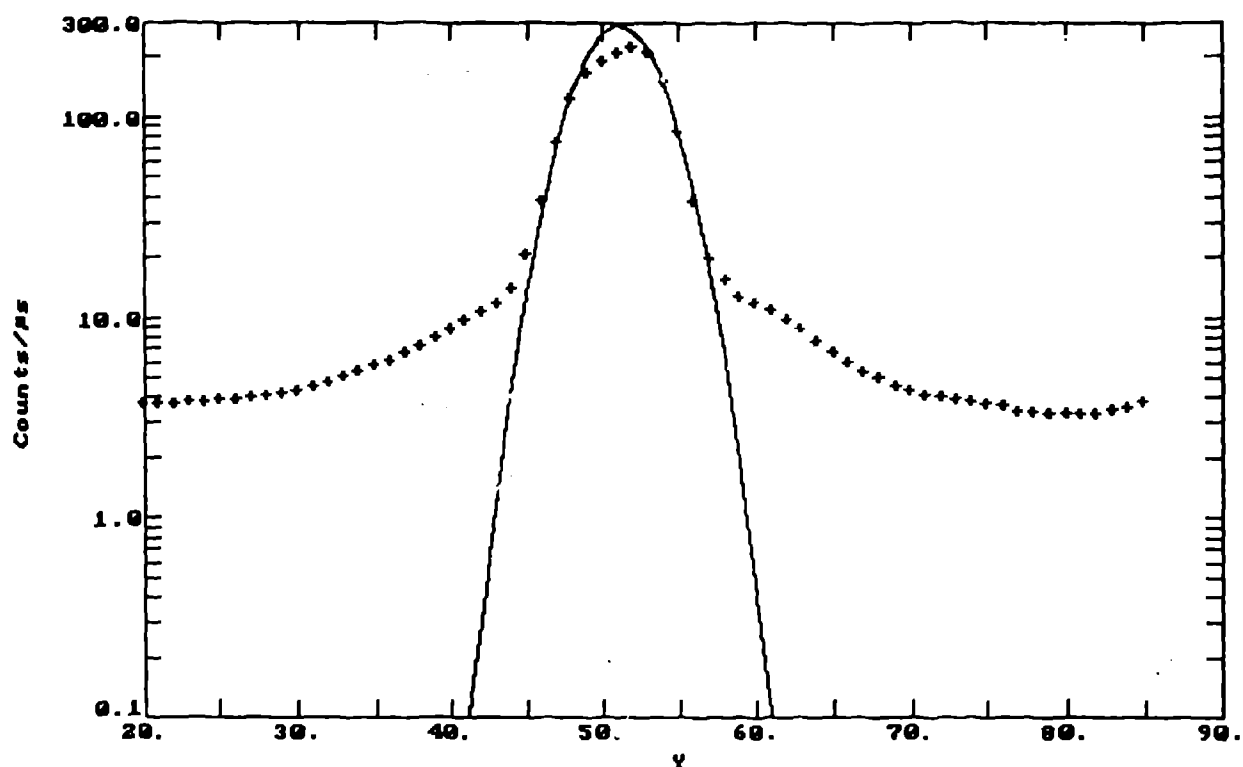


Fig. 5. Count rate as a function of vertical position, in the wavelength range 1.2 to 2.8 Å. The direct beam profile is estimated by the Gaussian; it is larger than and somewhat higher than the beam stop. In this range the scattering should be relatively isotropic.

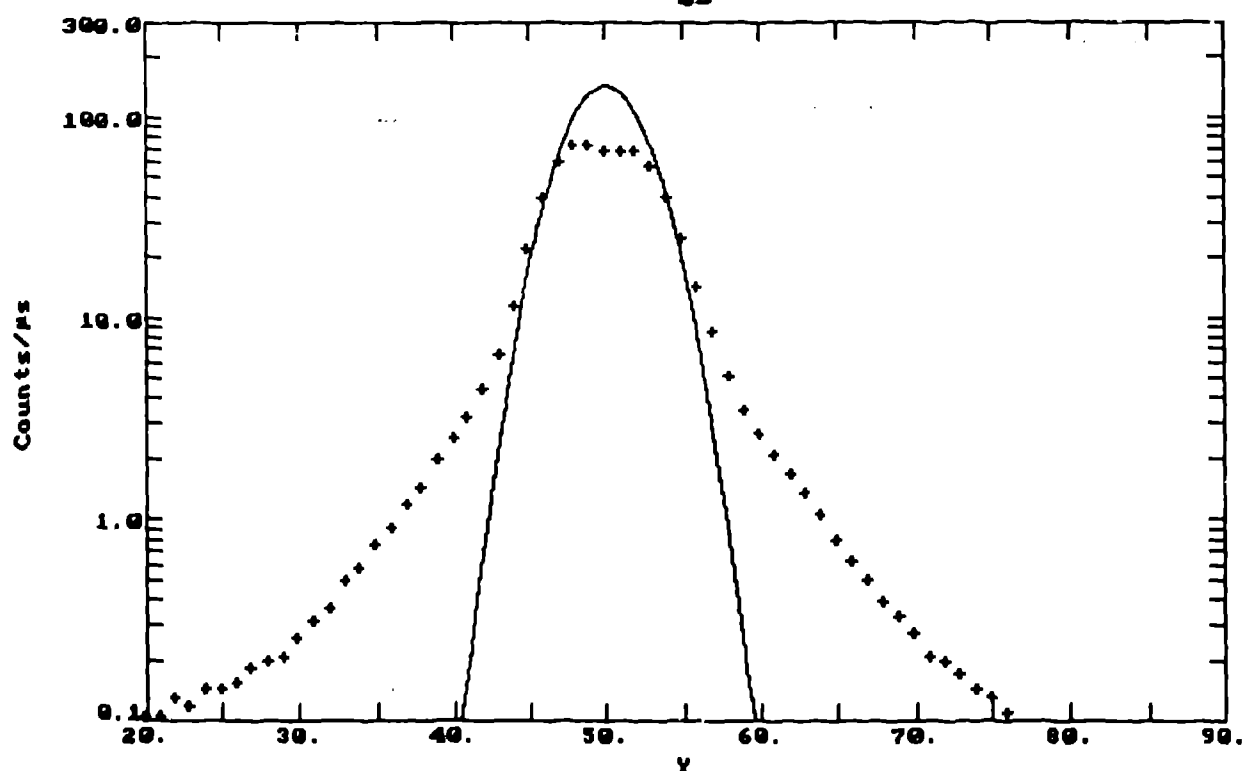


Fig. 6. Count rate as as function of vertical position, at  $\lambda = 12$  Å. At this time the beam has fallen far enough to be centered on the beam stop. Small-angle scattering from the 10-cm Pb sample is apparent.

### References

1. P. A. Seeger, A. Williams, and J. Trehella, Proceedings of the Eighth Meeting of the International Collaboration on Advanced Neutron Sources, report RAL-85-110, vol. 2, p. 441 (1985).
2. H. Robinson, G. J. Russell, K. D. Williamson Jr., and F. J. Edeskuty, AIChE Symposium Series 82 (1986) 172.
3. P. A. Seeger and M. J. Nutter, Proceedings of the Eighth Meeting of the International Collaboration on Advanced Neutron Sources, report RAL-85-110, vol. 3, p. 717 (1985).
4. P. A. Seeger, Physica 136B (1986) 106.
5. P. A. Seeger, Nucl. Instr. and Meth. 178 (1980) 157.
6. P. A. Seeger, IEEE Trans. Nucl. Sci. NS-31 (1984) 274.
7. J. K. Kjems, R. Bauer, B. Breiting, and A. Thuesen, in "Neutron Scattering in the 'Nineties", IAEA-CN-46 (1985) 489.
8. C. G. Windsor, "Pulsed Neutron Scattering" (Taylor & Francis, London, 1981) p. 261.